

# Histopathological and Immunohistochemical Features of Small to Big Satellite Nevus Uncover the Nevogenesis of Large/Giant Congenital Melanocytic Nevus

**Jieyu Gu**

Shanghai Jiao Tong University School of Medicine

**Boxuan Wei**

Shanghai Jiao Tong University School of Medicine

**Bowen Gao**

Shanghai Jiao Tong University School of Medicine

**Ran Duan**

Shanghai Jiao Tong University School of Medicine

**Lingling Sheng**

Shanghai Jiao Tong University School of Medicine

**Danning Zheng**

Shanghai Jiao Tong University School of Medicine

**Yongyang Bao**

Shanghai Jiao Tong University School of Medicine

**Feng Xie (✉ [xiefenghe@163.com](mailto:xiefenghe@163.com))**

Shanghai Jiao Tong University School of Medicine

---

## Research Article

**Keywords:** Nevogenesis, Large/ giant congenital melanocytic nevus, nevocyte, SOX10, p16, Ki67

**Posted Date:** May 31st, 2022

**DOI:** <https://doi.org/10.21203/rs.3.rs-1669887/v1>

**License:**   This work is licensed under a Creative Commons Attribution 4.0 International License.

[Read Full License](#)

---

# Abstract

The neovogenesis of large/giant congenital melanocytic nevus (IgCMN) is a complex biological process involving several integral prenatal stages. Limited by ethical concerns, the understanding of whether IgCMN develops from the epidermis to the dermis or in the opposite direction remains controversial. With the present study of the accompanying satellite nevi, we hypothesized that IgCMN developed from epidermis to dermis. The satellite nevi were subdivided into 3 groups: big (diameter > 10 mm), medium (> 5 mm but  $\leq$  10 mm), and small ( $\leq$  5 mm). Haematoxylin and eosin and immunohistochemical staining (SOX10, Ki67, p16) were performed to compare the nevocyte infiltration depth as well as the positive-stained cell proportions among these satellite nevi. In small satellite nevi, less deeply the nevocytes infiltrated the dermis, as well as more cells in the epidermis expressed SOX10 and Ki67 and fewer cells in the dermis expressed p16 than in big satellite nevi. Additionally, two specimens were obtained from each of 4 patients who underwent serial resections of IgCMN at an average interval of 1.75 years to examine the histopathological changes between them. In the present study, satellite nevi of different sizes represent different stages of IgCMN from early to late, deepening our comprehension of the sequential stages of IgCMN neovogenesis. Initially, abnormal nevocytes seeded, proliferated and spread along the epidermis. At specific locations, some nevocytes formed nests and gradually penetrated into the dermis. Eventually, the nevocytes infiltrated the dermis and entered a homeostatic state. This study provides new evidence supporting the theory of epidermal-to-dermal neovogenesis in IgCMN.

## Introduction

Large/giant congenital melanocytic nevi (IgCMNs) are melanocytic lesions that cover the skin extensively at birth. Based on the predicted maximal adult size (PAS), lesions between 20 and 40 cm are classified as LCMNs, and lesions larger than 40 cm are classified as GCMNs (Krengel et al. 2013). How nevocytes proliferate, migrate and aggregate in the epidermis/dermis and eventually form melanocytic nevi during embryonic development remains unclear.

Currently, there are two hypotheses regarding the process of neovogenesis (Grichnik 2008; Grichnik et al. 2014): (i) Unna's Abtropfung ('trickling down') hypothesis, where mutated melanocytes in the basal layer of the epidermis proliferate abnormally and descend gradually into the dermis; and (ii) Cramer's Hochsteigerung ('upward climbing') hypothesis, where mutated melanoblasts proliferate abnormally, occupy the dermis and finally form a nevus during migration towards the epidermis.

A study on neovogenesis demonstrated that acquired melanocytic nevus (AMN) formation follows the Abtropfung hypothesis (Wang et al. 2020), in which mutated melanocytes proliferate abnormally and descend into the dermis. The similarities between CMNs and AMNs are as follows: (i) the histopathological architecture between them is characterized by gradual decreases in nevocyte size, pigmentation, and cell aggregate size deep within the dermis; however, the nevocytes infiltrate more deeply in CMN (Yeh 2020); and (ii) CMN and AMN share the same global dermoscopic patterns and local features (Errichetti et al. 2017). Thus, we proposed that the neovogenesis of CMN follows the same

Abtropfung trickling down pattern as AMN. However, as a congenital disease, it is not feasible to observe the nevogenesis of IgCMN continuously in vivo because of experimental ethical and technical limitations. In this study, the accompanying satellite nevi of IgCMN provide a new model for nevogenesis research.

The satellite nevi of IgCMN exist in various numbers and sizes, ranging from tens of centimetres to a few millimetres (Yun et al. 2012; Kregel et al. 2013). Research has indicated that there might be homology between satellite nevi and the corresponding IgCMN because of a shared genetic mutation or fusion gene (Martins et al. 2019; Stark et al. 2021). On the other hand, it is known that nevocytes can be transported throughout the circulation because benign nevocytes were discovered in blood vessels, lymphatics and blood circulation in IgCMN (Schneider and Maie 1985; Barnhill et al. 2010; De Giorgi et al. 2012; Kokta et al. 2013). Accordingly, the nevocytes in satellite nevi may originate from a single mutated nevocyte in IgCMN, be transported to another skin site and develop into a nevus. The progression from a transported nevocyte to an aggregation of nevocytes in the epidermis/dermis of satellite nevi reiterates the nevogenesis of IgCMN during embryonic development. Via a histopathological investigation of satellite nevi of various sizes, our study should reveal the process of nevogenesis from a single mutated nevocyte to the formation of a nevus.

We conducted haematoxylin and eosin (H&E) and immunohistochemical (IHC) staining to reveal the histopathological pattern of IgCMNs and satellite nevi. SOX10, a transcription factor found in neural crest-derived cells, is indispensable for the specification, maturation, and maintenance of melanocytes (Shakhova et al. 2012); thus, it was used as a melanocytic lineage marker. Ki67, which is expressed only in cells with an active cell cycle, is a marker of proliferation (Miller et al. 2018). p16 is a cyclin-dependent kinase inhibitor that negatively regulates the cell cycle and inhibits cell proliferation (Rayess et al. 2012), and its expression is elevated in some melanocytic lesions (Michaloglou et al. 2005; Stefanaki et al. 2008; Uguan et al. 2018).

Since big satellite nevi develop incrementally from small nevi, the nevogenesis of IgCMN from early to late can be inferred from satellite nevi of various sizes. This study was intended to uncover the histopathological characteristics of satellite nevi of various sizes, including the distribution of SOX10-positive cells, as well as the expression of the proliferation marker Ki67 and the cell cycle inhibitor p16, to reveal the nevogenesis from a single mutated nevocyte to IgCMN during embryonic development.

## Materials And Methods

### Selection of Patients and Specimens

Nineteen satellite nevi samples from 7 patients and thirty-nine IgCMN samples from 31 patients were included. For 4 patients, two IgCMN samples were harvested at different times, with an average interval of 1.75 years. All satellite nevi samples were classified into 3 groups: big (diameter >10 mm), medium (>5 mm but ≤10 mm), and small (≤5 mm). All specimens were previously fixed in formalin and embedded in paraffin, and 4-µm-thick sections were obtained for H&E and IHC staining. The study was approved by the Ethics Committee of Shanghai Ninth People's Hospital (Shanghai, China).

## **H&E Staining and Evaluation of the Nevocyte Infiltration Depth**

Tissue sections were stained with H&E to examine the histopathological architecture, especially the nevocyte infiltration depth. To determine the infiltration depth in the dermis, H&E-stained sections of satellite nevi were observed under a microscope (Leica, Wetzlar, Germany) in a low-power field. Micrographs were taken using Image-Pro Plus 6.0 software (Media Cybernetics, Silver Spring, MD, USA). The nevocyte infiltration depth, defined as the maximum distance from the nevocytes at the dermal-epidermal junction (DEJ) to the deepest involvement in the dermis, was measured in microns. The results were derived from five randomly selected fields in each satellite nevi section.

## **IHC Staining**

After deparaffinization and hydration, the sections were subjected to melanin bleaching (0.25% potassium permanganate for 1 minute and 0.5% oxalic acid for 1 minute) because excessive melanin would conceal the staining results. Heat-mediated antigen retrieval and blocking of endogenous peroxidase and nonspecific binding were performed according to the manufacturer's protocol. Then, the sections were incubated with primary antibodies against SOX10 (Abcam, ab227680, 1:100), Ki67 (Maxim, MX006, 1:200), and p16 (Maxim, MX007, 1:200) at 37 °C for 1 hour. Then, the samples were incubated with an HRP-conjugated secondary antibody (Abcam, ab205718 for anti-rabbit, ab205719 for anti-mouse) at room temperature for 30 minutes and were then visualized using 3,3'-diaminobenzidine (DAB) as a chromogen. Some sections contained vast amounts of melanin; thus, the red chromogen 3-amino-9-ethylcarbazole (AEC) was used on these sections instead. Nuclei were counterstained with haematoxylin. The sections were observed under a light microscope and recorded digitally. For double immunofluorescence staining, FITC-conjugated goat anti-rabbit IgG (Abcam, ab6717) and Cy3-conjugated goat anti-mouse IgG (Abcam, ab97035) were used as secondary antibodies. These sections were imaged under a fluorescence microscope (Olympus, Tokyo, Japan).

## **Evaluation of IHC Staining**

The immunostained sections were analysed and counts were made of cells that were positive for SOX10, Ki67 and p16 by microscopic examination at 400× magnification. The proportions of positively stained cells were calculated by dividing the number of positive cells by the total number of cells in each field. For each case, the average proportion of positive cells was calculated in 5 fields. As the cell density was different between the superficial and deep dermis, these areas were assessed separately.

## **Statistical analysis**

A nonparametric Kruskal–Wallis test (for >2 unpaired groups) was applied to compare the proportion of SOX10- or Ki67-positive cells in the epidermis between big, medium and small satellite nevi. The Mann–Whitney U test was used to analyse the difference between two groups (such as the proportion of p16-positive cells in the dermis of IgCMN and satellite nevi). Differences were considered statistically significant if the p value was < 0.05.

# Results

## **Nevogenesis progressed from the epidermis to the dermis**

IHC staining of SOX10 in the smallest satellite nevus (2 mm in diameter) included in the study demonstrated that SOX10-positive cells were distributed in the epidermis but rarely deposited in the dermis, supporting the hypothesis that nevocytes first proliferate and spread in the epidermis (Fig. 1A). There were nests composed of aggregated nevocytes at the DEJ. SOX10 and Ki67 staining of serial sections verified the presence of Ki67-positive cells in these nevocyte nests, suggesting cell proliferation in the nests (Fig. 1B). The SOX10-positive cells in the dermis were associated with sweat glands, one of the histopathological features of CMN. The nests then penetrated the basal layer of the epidermis and infiltrated into the dermis while expanding. As a result, increased nevocytes and melanin were deposited in the dermis but were still limited to the superficial layer. Gradually, the nests dispersed into the deep dermis, resulting in a gradient distribution of nevocytes, with a high density in the superficial dermis and a low density in the deep dermis (Fig. 1C). In addition, the presence of nevocyte nests in the dermis was examined among patients of different ages. The results showed that IgCMN patients without nests in the dermis appeared to be significantly older (Fig. 1D).

## **Satellite nevi of various sizes represented the dynamics of nevogenesis**

The infiltration depth of nevocytes varied with the size of satellite nevi (Fig. 2). In small satellite nevi, nevocytes were mainly located at the DEJ, with a low density. Medium satellite nevi exhibited a higher density of nevocytes at the DEJ and had dispersed nevocytes in the deep dermis. In addition to melanin being present in the basal layer of the epidermis, intradermal nevocytes also secrete melanin. In big satellite nevi, nevocytes not only penetrated more deeply but also had a higher density and more melanin. It can be concluded that the bigger the satellite nevus was, the more deeply the nevocytes infiltrated. IHC staining revealed that the average percentages of SOX10-positive cells in the epidermis of small, medium, and big satellite nevi were 11.66%, 7.87% and 7.23%, respectively ( $p > 0.05$ , Fig. 3, Table 1). The percentages of Ki67-positive cells in the epidermis were 6.85%, 3.43% and 3.47%, respectively ( $p < 0.05$ , Fig. 3, Table 1). The smaller the satellite nevus was, the more Ki67-positive cells were in the epidermis. The percentage of p16-positive cells in the dermis was 26.98% in the big satellite nevi group and 14.80% in the medium satellite nevi group ( $p < 0.05$ , Fig. 3, Table 1). A comparison of the p16-positive cell proportion in the small group was excluded due to the rarity of cells in the dermis. Furthermore, double immunofluorescence staining of SOX10 and p16 between big satellite nevi and IgCMN revealed that p16-positive nevocytes in the dermis of satellite nevi were significantly fewer than those in IgCMN (15.87% and 23.58% in big satellite nevi and IgCMN, respectively, Fig. 4).

## **IgCMN eventually reached a homeostatic state**

Postnatally, the sizes of IgCMNs only increase with the growth and development of patients. The photos of Patient 1 taken at the ages of 5 and 7 showed no spreading of the nevus border. The IHC staining results were consistent with the clinical findings (Fig. 5A). The specimens harvested from two separate

surgeries at a 2-year interval exhibited no significant change in the proportion of SOX10-positive cells in either the epidermis or the dermis. In addition, there was no significant change in the proportion of p16-positive cells in the dermis. The proportions of SOX10-positive cells in the dermis were compared in the other three patients who had also undergone two surgeries, and no significant difference was found (Fig. 5B).

## Discussion

The controversy surrounding the hypotheses on nevogenesis focuses on whether nevocytes are first generated in the epidermis and then infiltrate deeper into the dermis (Abtropfung pattern) or whether lesions develop from deep to superficial during the migration and differentiation of neural crest cells (Hochsteigerung pattern). It is generally accepted that most IgCMNs are intradermal nevi, in which a large number of nevocytes are involved in the dermis and rarely in the epidermis. Kinsler (2013) observed a normal melanocyte population overlying many CMNs. It was also reported that a subepidermal noninvolvement zone lay at the DEJ in IgCMN, and no abnormal nevocytes were discovered in the epidermis (Wu 2018). These results support the idea that IgCMNs originate in the dermis. However, our study showed the opposite results, and we believe that the nevogenesis of IgCMNs commences in the epidermis.

In addition, our study confirmed a histopathological similarity between satellite nevi and IgCMN (Fig. S1; see Supplementary Information). Thus, it was inferred that the nevogenesis of satellite nevi is the same as that of IgCMN in embryos, except that satellite nevi develop later than IgCMN, so they are smaller than IgCMN. Combined with previous findings of nevocytes in the blood or lymphatic vessels and the systemic circulation (Grichnik 2008; Grichnik et al. 2014; Wang 2020; Yeh 2020), our findings indicate that nevocytes in IgCMN could migrate through the systemic circulation to a distant skin location, where they would proliferate and eventually form satellite nevi during embryonic development. Therefore, this study should reveal the process of IgCMN development by examining the histopathological features of small, medium and big satellite nevi.

The smallest satellite nevus (2 mm in diameter) in this study exhibited distributed nevocytes along the epidermis and few nevocytes in the dermis (Fig. 1A), which is consistent with a previous study where abnormal melanocytes were focally clustered in the rete ridges of the epidermis in an 18-week-old aborted embryo (Cramer and Fesyuk 2012). Accordingly, our study indicates that abnormal nevocytes first colonize and spread along the basal layer during the early stage of nevogenesis, which supports the hypothesis that nevogenesis begins from the epidermis. Then, some nevocytes proliferate and form nests composed of aggregated nevocytes. IHC staining showed that almost all cells in the nests were positive for SOX10, and a few of them were positive for Ki67, indicating that nevocytes in the nests could proliferate (Fig. 1B). As the nest grows more prominent, it gradually penetrates towards the dermis until the entire nest descends and disperses into the dermis (Fig. 1C). The capability of nevocytes to migrate deeply into the dermis may be related to their escape from the control of keratinocytes (Gontier et al.

2004; Matsuda et al. 2008), which is the second step in nevogenesis. However, how nevocytes acquire this ability requires further study.

Based on their diameter, satellite nevi were classified as big (> 10 mm), medium (> 5 mm but ≤ 10 mm) and small (≤ 5 mm). The infiltration depth of nevocytes varied with the sizes of satellite nevi. The larger the satellite nevus was, the more deeply nevocytes infiltrated, supporting the dynamics of nevogenesis from superficial to deep. IHC staining of SOX10 and Ki67 demonstrated that the smaller the satellite nevus was, the more Ki67-positive cells were in the epidermis, indicating that small satellite nevi were in the proliferative phase, which might correspond to the early stage of IgCMN development. p16 staining in the medium and big satellite nevi groups indicated that the bigger the satellite nevus was, the more cells expressed p16, indicating a state of cell cycle inhibition, which supports the hypothesis that satellite nevi of various sizes represent the dynamics of nevogenesis from early to late. Double immunofluorescence staining of p16 and SOX10 in big satellite nevi and IgCMN revealed more cell cycle-inhibited nevocytes in IgCMN than in satellite nevi (Fig. 4). The expression of p16 may contribute to the homeostatic state of IgCMNs, where the lesions no longer evidently grow. However, the underlying mechanism needs further study.

To further prove the homeostatic state of IgCMN, we examined the proportions of SOX10- and p16-positive cells in both the epidermis and dermis, which did not change significantly between two separate specimens from the same patient at an interval of 2 years. Combined with the above results, it was concluded that IgCMN eventually reached a homeostatic state, where the population and the component ratio of nevocytes remained stable.

From this histopathological study of IgCMN and satellite nevi of various sizes, we support the hypothesis that nevogenesis begins in the epidermis (Fig. 6). First, nevocytes abnormally proliferate and spread along the basal layer of the epidermis. At features such as rete ridges in the epidermis, some nevocytes aggregate, forming nests, which gradually expand and disperse into the dermis. During development, the number of Ki-67-positive cells decreases gradually, which means that their proliferation ability gradually decreases. Meanwhile, the expression of p16 in nevocytes in the dermis steadily increases, indicating a restraint on nevocyte proliferation, which results in a balance in the number of nevocytes. Eventually, the nevus reaches a homeostatic state. This study provides new evidence for the theory of epidermal-to-dermal nevogenesis in IgCMN.

## Declarations

All authors have participated the study and approved the final manuscript. The authors have no relevant financial or non-financial conflicts of interest to disclose. This work was supported by the National Natural Science Foundation of China (No. 81871595), the Scientific Research Project of Shanghai Municipal Health Commission (No. 202040432), the Cross Research Fund Project of Shanghai Ninth People's Hospital, Shanghai JiaoTong University School of Medicine (No. JYJC201903).

## Data Availability Statement

All data generated or analysed during this study are included in this published article (and its supplementary information files).

## Funding Declaration

This work was supported by the National Natural Science Foundation of China (No. 81871595), the Scientific Research Project of Shanghai Municipal Health Commission (No. 202040432), the Cross Research Fund Project of Shanghai Ninth People's Hospital, Shanghai JiaoTong University School of Medicine (No. JYJC201903).

## Conflict of Interest

The authors have no relevant financial or non-financial conflicts of interest to disclose.

## Ethical approval

The study was approved by the Ethics Committee of Shanghai Ninth People's Hospital (Shanghai, China). Formal consent was not required because the clinical information is anonymized and the images does not contain information that may identify the person.

## References

1. Barnhill RL, Chastain MA, Jerdan MS, Lebbé C, Janin A, Lugassy C. Angiotropic neonatal congenital melanocytic nevus: how extravascular migration of melanocytes may explain the development of congenital nevi. *Am J Dermatopathol*. 2010;32(5):495–499. <https://doi.org/10.1097/DAD.0b013e3181c6afce>
2. Cramer SF, Fesyuk A. On the development of neurocutaneous units—implications for the histogenesis of congenital, acquired, and dysplastic nevi. *Am J Dermatopathol*. 2012;34(1):60–81. <https://doi.org/10.1097/DAD.0b013e31822d071a>
3. De Giorgi V, Pinzani P, Salvianti F, et al. Circulating benign nevus cells detected by ISET technique: warning for melanoma molecular diagnosis. *Arch Dermatol*. 2010;146(10):1120–1124. <https://doi.org/10.1001/archdermatol.2010.264>
4. Errichetti E, Patriarca MM, Stinco G. Dermoscopy of congenital melanocytic nevi: a ten-year follow-up study and comparative analysis with acquired melanocytic nevi arising in prepubertal age. *Eur J Dermatol*. 2017;27(5):505–510. <https://doi.org/10.1684/ejd.2017.3088>
5. Gontier E, Cario-André M, Vergnes P, Lepreux S, Surlève-Bazeille JE, Taïeb A. The role of E-cadherin in nevogenesis: an experimental study using epidermal reconstructs. *Exp Dermatol*. 2004;13(5):326–331. <https://doi.org/10.1111/j.0906-6705.2004.00155.x>
6. Grichnik JM. Melanoma, nevogenesis, and stem cell biology. *J Invest Dermatol*. 2008;128(10):2365–2380. <https://doi.org/10.1038/jid.2008.166>

7. Grichnik JM, Ross AL, Schneider SL, Sanchez MI, Eller MS, Hatzistergos KE. How, and from which cell sources, do nevi really develop?. *Exp Dermatol*. 2014;23(5):310–313. <https://doi.org/10.1111/exd.12363>
8. Kinsler VA, Anderson G, Latimer B, et al. Immunohistochemical and ultrastructural features of congenital melanocytic naevus cells support a stem-cell phenotype. *Br J Dermatol*. 2013;169(2):374–383. <https://doi.org/10.1111/bjd.12323>
9. Kokta V, Hung T, Al Dhaybi R, Lugassy C, Barnhill RL. High prevalence of angiotropism in congenital melanocytic nevi: an analysis of 53 cases. *Am J Dermatopathol*. 2013;35(2):180–183. <https://doi.org/10.1097/DAD.0b013e318260908c>
10. Krengel S, Scope A, Dusza SW, Vonthein R, Marghoob AA. New recommendations for the categorization of cutaneous features of congenital melanocytic nevi. *J Am Acad Dermatol*. 2013;68(3):441–451. <https://doi.org/10.1016/j.jaad.2012.05.043>
11. Martins da Silva V, Martinez-Barrios E, Tell-Martí G, et al. Genetic Abnormalities in Large to Giant Congenital Nevi: Beyond NRAS Mutations. *J Invest Dermatol*. 2019;139(4):900–908. <https://doi.org/10.1016/j.jid.2018.07.045>
12. Matsuda N, Katsube K, Mikami S, et al. E-cadherin expression in the subepithelial nevus cells of the giant congenital nevocellular nevi (GCNN) correlates with their migration ability in vitro. *J Dermatol Sci*. 2008;52(1):21–30. <https://doi.org/10.1016/j.jdermsci.2008.04.001>
13. Michaloglou C, Vredeveld LC, Soengas MS, et al. BRAFE600-associated senescence-like cell cycle arrest of human naevi. *Nature*. 2005;436(7051):720–724. <https://doi.org/10.1038/nature03890>
14. Miller I, Min M, Yang C, et al. Ki67 is a Graded Rather than a Binary Marker of Proliferation versus Quiescence. *Cell Rep*. 2018;24(5):1105–1112.e5. <https://doi.org/10.1016/j.celrep.2018.06.110>
15. Rayess H, Wang MB, Srivatsan ES. Cellular senescence and tumor suppressor gene p16. *Int J Cancer*. 2012;130(8):1715–1725. <https://doi.org/10.1002/ijc.27316>
16. Schneider BV, Maie O. The ultrastructure of congenital nevocytic nevi. I. Nevus cells in walls of blood vessels and lymphatics. *Arch Dermatol Res*. 1985;278(1):49–56. <https://doi.org/10.1007/BF00412496>
17. Shakhova O, Zingg D, Schaefer SM, et al. Sox10 promotes the formation and maintenance of giant congenital naevi and melanoma. *Nat Cell Biol*. 2012;14(8):882–890. <https://doi.org/10.1038/ncb2535>
18. Stark MS, Tell-Martí G, Martins da Silva V, et al. The Distinctive Genomic Landscape of Giant Congenital Melanocytic Nevi. *J Invest Dermatol*. 2021;141(3):692–695.e2. <https://doi.org/10.1016/j.jid.2020.07.022>
19. Stefanaki C, Stefanaki K, Antoniou C, et al. G1 cell cycle regulators in congenital melanocytic nevi. Comparison with acquired nevi and melanomas. *J Cutan Pathol*. 2008;35(9):799–808. <https://doi.org/10.1111/j.1600-0560.2007.00912.x>
20. Uguen A, Uguen M, Guibourg B, Talagas M, Marcorelles P, De Braekeleer M. The p16-Ki-67-HMB45 Immunohistochemistry Scoring System is Highly Concordant With the Fluorescent In Situ

Hybridization Test to Differentiate Between Melanocytic Nevi and Melanomas. Appl Immunohistochem Mol Morphol. 2018;26(6):361–367.  
<https://doi.org/10.1097/PAI.0000000000000428>

21. Wang DG, Huang FR, Chen W, et al. Clinicopathological Analysis of Acquired Melanocytic Nevi and a Preliminary Study on the Possible Origin of Nevus Cells. Am J Dermatopathol. 2020;42(6):414–422.  
<https://doi.org/10.1097/DAD.0000000000001599>
22. Wu M, Yu Q, Gao B, Sheng L, Li Q, Xie F. A large-scale collection of giant congenital melanocytic nevi: Clinical and histopathological characteristics. Exp Ther Med. 2020;19(1):313–318.  
<https://doi.org/10.3892/etm.2019.8198>
23. Yeh I. New and evolving concepts of melanocytic nevi and melanocytomas. Mod Pathol. 2020;33(Suppl 1):1–14. <https://doi.org/10.1038/s41379-019-0390-x>
24. Yun SJ, Kwon OS, Han JH, et al. Clinical characteristics and risk of melanoma development from giant congenital melanocytic naevi in Korea: a nationwide retrospective study. Br J Dermatol. 2012;166(1):115–123. <https://doi.org/10.1111/j.1365-2133.2011.10636.x>

## Tables

**Table 1. Percentages of positive-stained cells in the epidermis/ dermis of IgCMN and satellite nevi in various sizes.**

	IgCMN	Satellite Nevus			p value
		Big	Medium	Small	
<b>SOX10% in Epidermis</b>	5.14	8.75			–
		7.23	7.87	11.66	p >0.05
<b>Ki67% in Epidermis</b>	4.24	5.47			–
		3.47	3.43	6.85	p <0.05
<b>p16% in Dermis</b>	–	–			–
		26.98	14.80	–	p <0.05
<b>p16/SOX10% in Dermis</b>	24.31	17.26			p <0.05
		–	–	–	

## Figures

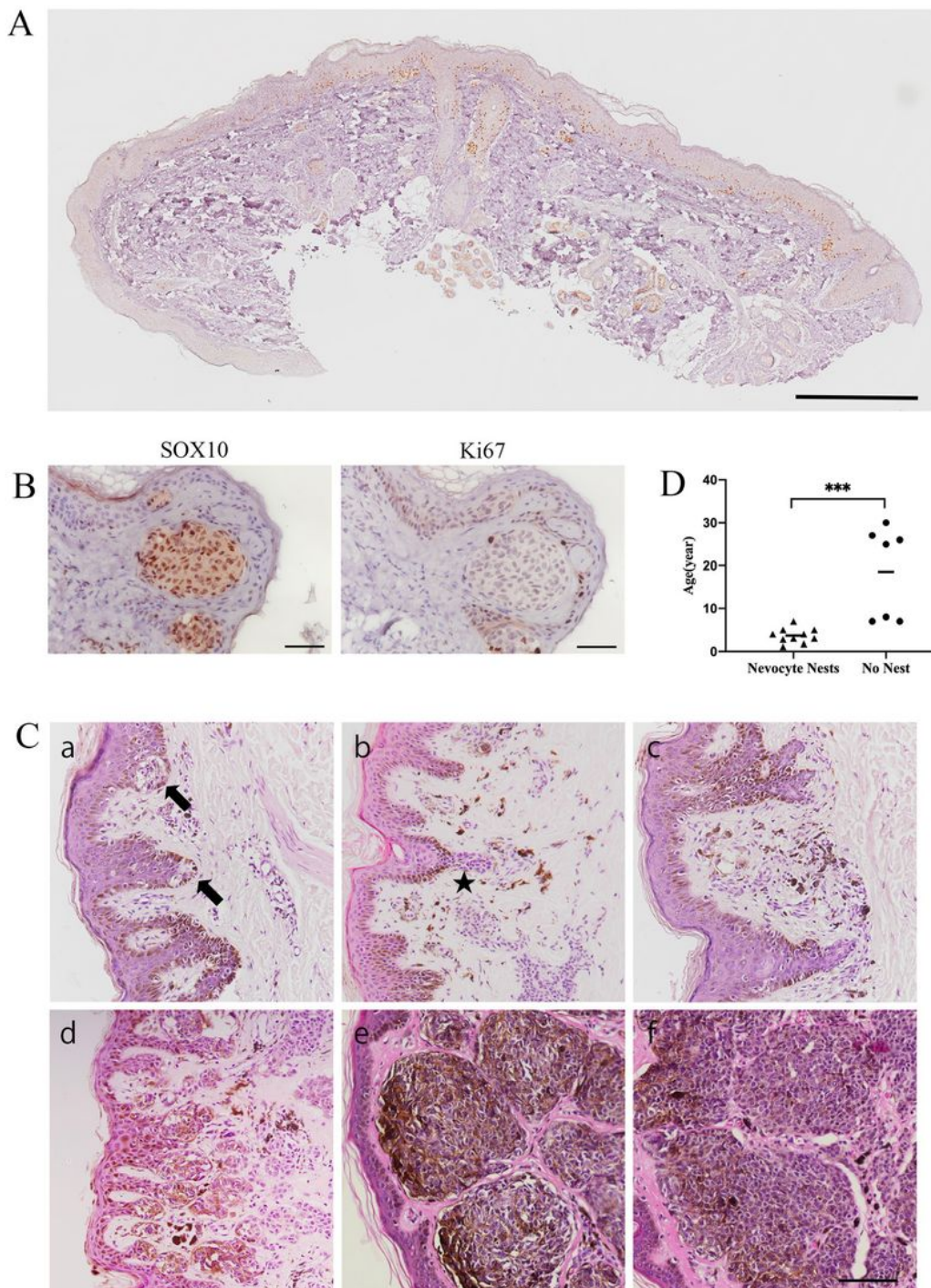


**Figure 1**

Nevi developed from the epidermis to the dermis. (A) IHC staining of SOX10 in the smallest nevus included in this study (scale bar = 100  $\mu$ m). (B) IHC staining of SOX10 and Ki67 in nevocystic nests in serial sections (scale bar = 50  $\mu$ m). (C) a. Nevocystic nests (indicated by the arrows) in the epidermal rete ridges and few nevocytes in the dermis of small satellite nevi; b. The nevocystic nests expanded towards the dermis (indicated by the star); c. Nevocytes and melanin in the dermis of satellite nevi but were limited

to the superficial dermis; d. A large number of nests penetrated the dermis; e. Large nests in the dermis; f. Dispersed nevocyttes and melanin in the dermis (H&E; scale bar = 100  $\mu$ m). (D) IgCMN patients without nests in the dermis appeared to be significantly older than those with nests in the dermis (\*\*\*) represents a p value = 0.0002).

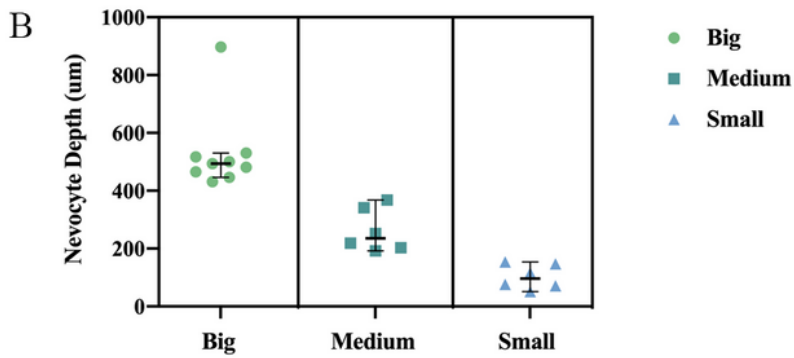
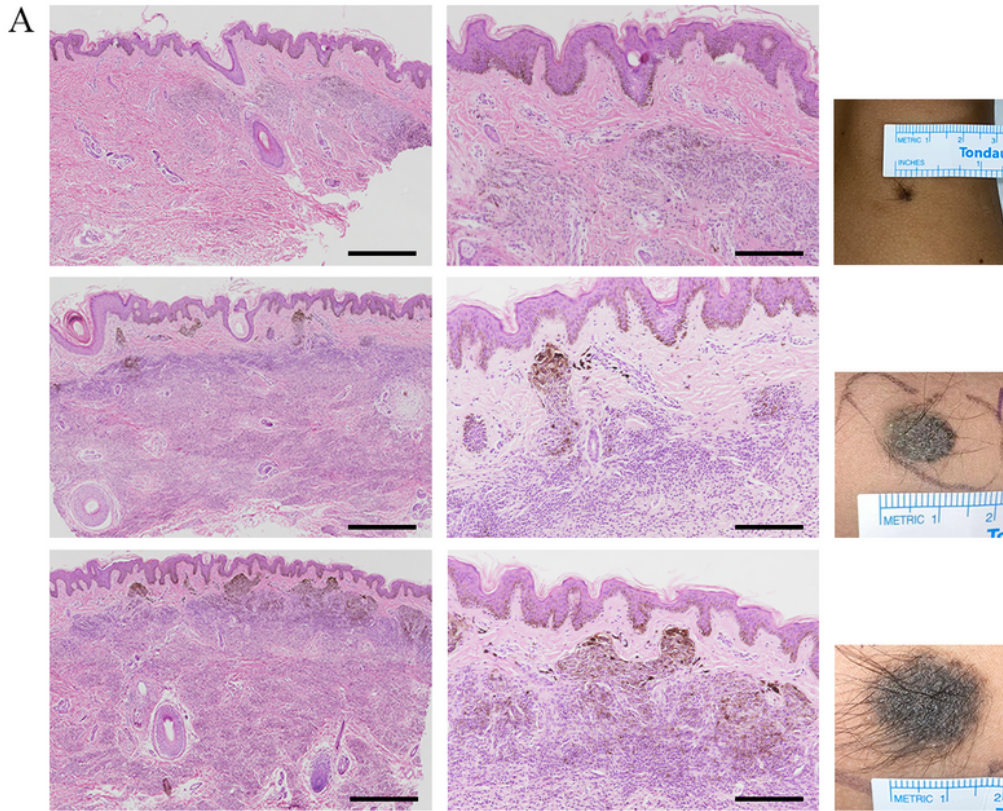


Figure 2

According to size (from small to big), satellite nevi infiltrated the dermis from superficial to deep. (A) H&E staining and clinical images of satellite nevi from small to big; the bigger the satellite nevus was, the deeper in the dermis where the nevocytes were deposited, with more melanin accumulated at the DEJ (scale bar = 500  $\mu$ m in the first column and 200  $\mu$ m in the second column; DEJ, dermal-epidermal junction). (B) The nevocyte infiltration depth of big, medium, and small satellite nevi.

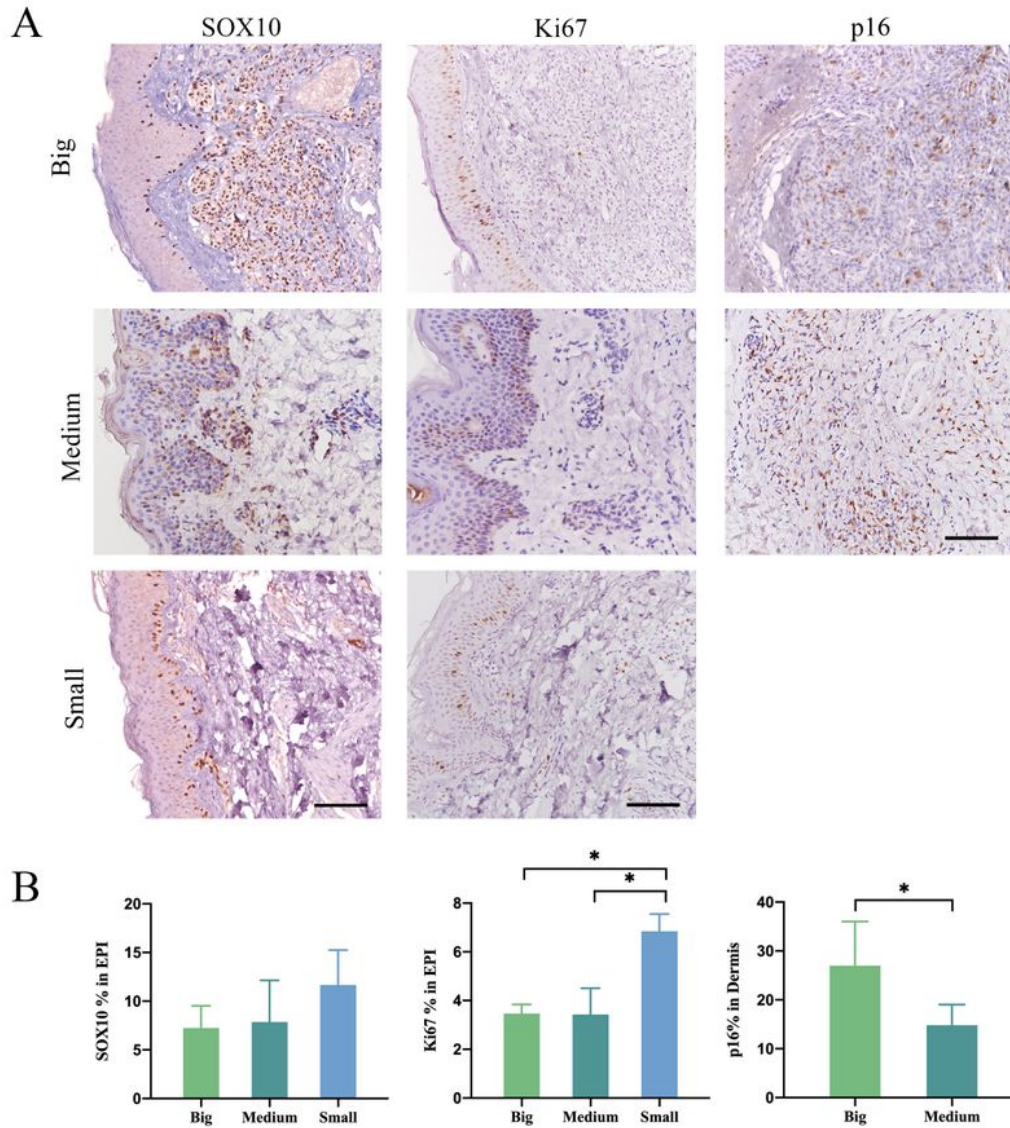
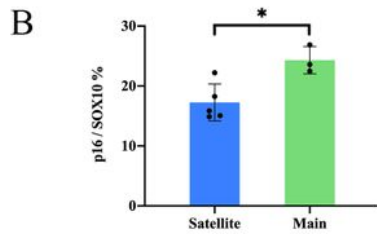
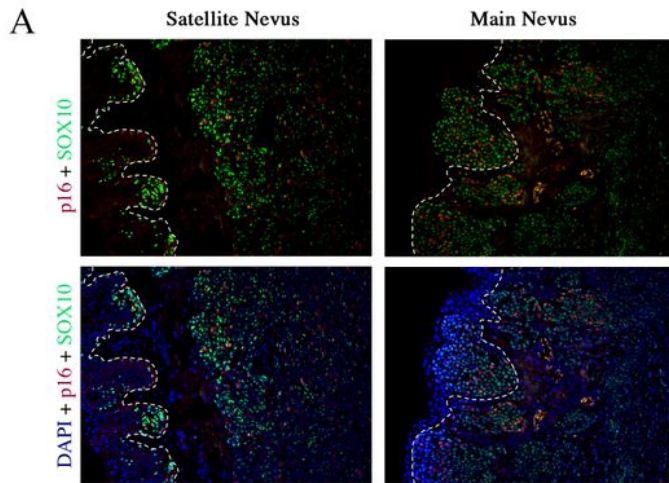


Figure 3

IHC staining of SOX10, Ki67 and p16 varied among big, medium and small satellite nevi. (A) IHC staining of SOX10, Ki67 and p16 in big, medium and small satellite nevi (scale bar = 100  $\mu$ m). (B) The proportions of cells that were positive for SOX10, Ki67 and p16 were compared among big, medium and small satellite nevi (\* represents a p value < 0.05).



## Figure 4

More nevocytes in IgCMN expressed p16 than in big satellite nevi. (A) Double immunofluorescence staining of SOX10 and p16 in IgCMNs and big satellite nevi (blue, DAPI; green, SOX10; red, p16; scale bar = 200  $\mu\text{m}$ ). (B) Proportions of SOX10 and p16 double-positive cells were compared between IgCMN and big satellite nevi (\* represents a p value < 0.05).

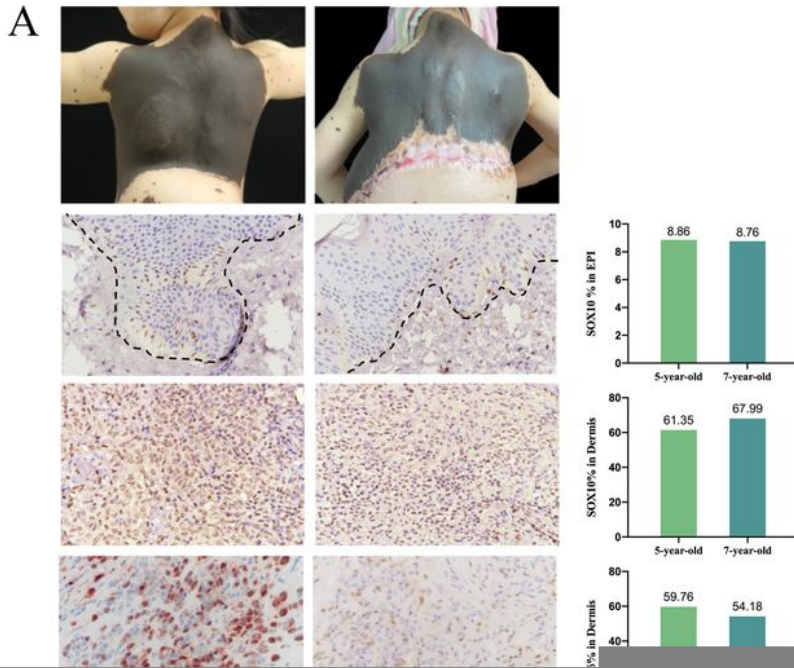


**Figure 5**

IgCMNs eventually reached a homeostatic state. (A) Clinical images and IHC staining of SOX10 and p16 in sections obtained from one patient at the ages of 5 (first column) and 7 (second column) years. The proportions of SOX10-positive cells in the epidermis and dermis and of p16-positive cells in the dermis were compared ( $p$  value  $> 0.05$ ). (B) Comparison of the proportions of SOX10-positive cells in the dermis obtained from four patients during two surgeries ( $p$  value  $> 0.05$ ).

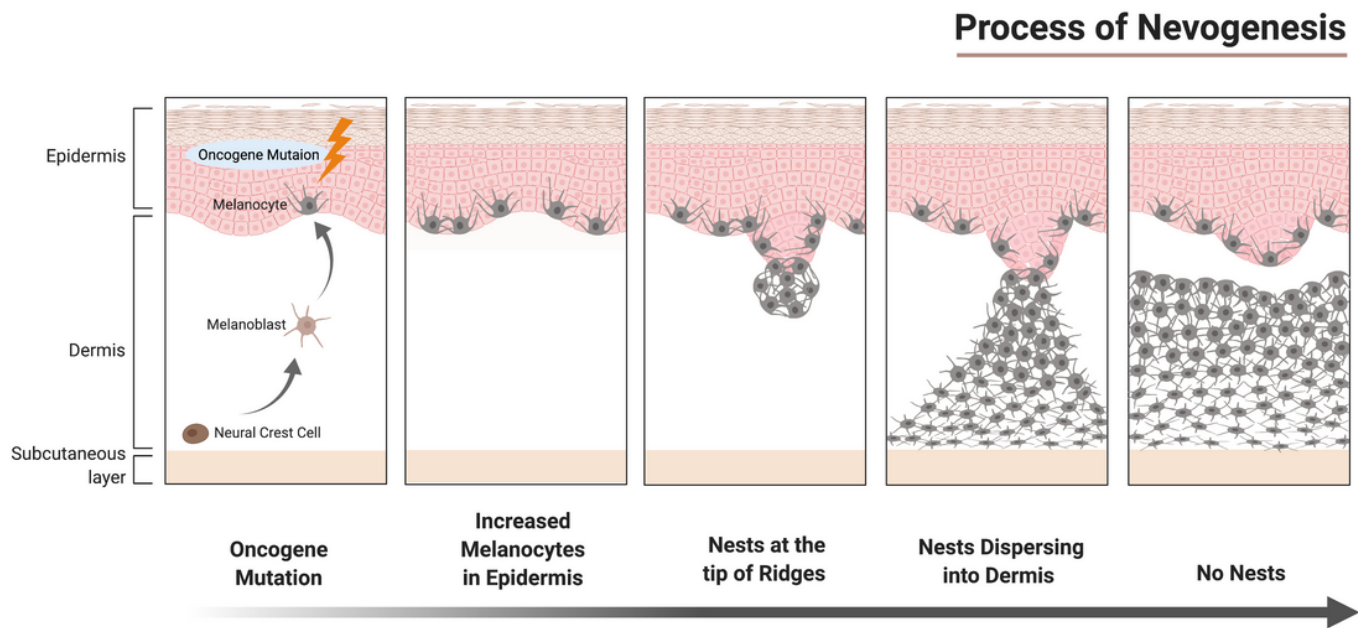


**Figure 6**

Schematic illustration of nevogenesis (Created with BioRender). The mutated melanocyte first colonizes and proliferates along the basal layer of the epidermis, after which some of the nevocytes proliferate and form nests composed of aggregated nevocytes. As the nest grows more prominent, it gradually penetrates and disperses the dermis, forming a high density of round-shaped nevocytes in the superficial dermis and a low density of spindle-shaped nevocytes in the deep dermis.

## Supplementary Files

This is a list of supplementary files associated with this preprint. Click to download.

- [FigS1.jpg](#)
- [TableS1.docx](#)